International Journal of Applied Mathematics in Control Engineering 6 (2023) 117-123

Contents lists available at YXpublications

International Journal of Applied Mathematics in Control Engineering

Journal homepage: http://www.ijamce.com

Hierarchical Classification Method for Subsurface Pipe Image Based on Resnet18 Transfer Learning

Zhaopeng Deng[a], Shuangyang Han[a], Hao Wen[a], Guangfen Zhang[b,*]

[a] College of Information and Control Engineering, Qingdao University of Technology, Qingdao 266525, China

[b] Data Science School, Qingdao Huanghai University, Qingdao 266427, China

ARTICLE INFO

Article history:
Received 5 April 2023
Accepted 10 May 2023
Available online 12 May 2023

Keywords:
image classification
Transfer learning
ResNet18
Subsurface pipe desalination

ABSTRACT

In response to issues such as the limited sample size of images for subsurface salt discharge pipes in saline-alkali land and the lack of an assessment mechanism for internal anomalies, this paper proposes a hierarchical classification method for subsurface pipes image based on ResNet18 transfer learning. This method adopts the strategy of data layering to label the dataset in a hierarchical manner, allowing for a more detailed classification of subsurface pipe images. It enables accurate assessments of the severity of subsurface pipe issues in saline-alkali lands based on the accumulation of sediments and salt crystals. Additionally, leveraging pre-trained networks with transfer learning significantly reduces the requirement for sample quantities during network training and enhances the model performance in recognizing features in subsurface pipe images. To validate the effectiveness of the proposed method, comparative experiments were conducted with transfer-learning-based pre-trained models, including AlexNet, MobileNet_V3, and ShuffleNet_V2. The experimental results indicate that the classification accuracy of the deep learning transfer model based on ResNet18 is 90.52%. The precision, recall, and F1 score are 90.70%, 90.69%, and 90.69%, respectively. Compared to other pre-trained models, this method not only attains higher recognition accuracy but also showcases superior stability. Comprehensive experiments and reliability analysis indicate that the proposed classification method exhibits good robustness and generalization performance. It can be employed for the rapid and intelligent identification of underground salt discharge pipe images.

1. Introduction

Soil salinization is a significant global issue, impacting both the environment and livelihoods (Zhang et al., 2022). Soil improvement methods for saline-alkali land (Cui et al., 2023; Chen and Cao et al., 2022) include various measures such as agronomic practices, chemical agents, biological improvement, and hydraulic engineering. Among these, subsurface drainage for salt discharge is an effective hydraulic method for ameliorating saline-alkali land (Liu et al., 2021; Yang et al., 2022). Its principle is based on the hydro-salt movement rule of "salt comes with water, salt goes with water." By burying subsurface pipes with small holes at a depth of 1 to 2 meters below the ground surface and combining it with irrigation and leaching, it dissolves and drains the salt in the topsoil. However, for subsurface pipes in deeply buried saline-alkali land, monitoring, cleaning, and maintenance pose considerable challenges (Piciarelli et al., 2018; Xu et al., 2022). Over time, issues such as sediment accumulation and salt crystal deposition are prone to occur in these subsurface pipes. Once a section of the subsurface pipe system experiences severe soil accumulation and salt crystal precipitation, it may adversely impact the normal operation of the entire subsurface pipe system. Therefore, real-time detection of abnormal conditions within the subsurface pipes is an important link in ensuring the normal operation of the subsurface pipe system and preventing potential safety hazards. This real-time detection can quickly identify abnormalities within the subsurface pipes, allowing timely implementation of corresponding measures to ensure the stable operation of the subsurface pipe system (Huang et al., 2023).

Subsurface pipe detection is typically performed by using intelligent pipeline inspection tools for real-time monitoring. It identifies, locates, and quantifies defects and damage in the pipeline during normal operation, providing a foundation for scientific pipeline safety management. Through a thorough analysis of the inspection results, operators can gain detailed insights into the conditions of pipe wall corrosion, cracks, blockages, deformations, and other defects. Based on the examination findings, they can assess the integrity of the pipeline. In recent years, with the development of

* Corresponding author.
E-mail addresses: zhanggf1@126.com (G. Zhang)
doi:

the combination of pipeline inspection and machine vision, many researchers have attempted to utilize automated image recognition technology to identify and classify pipeline issues in the abundant image and video data generated after inspections (Yang et al., 2019; Liu et al., 2020). Image recognition typically refers to the use of computer processing and analysis of images to achieve understanding and discrimination of different image categories. Its principle is based on some measurement method, criterion, or metric to categorize the image to be recognized into a predefined pattern class (Kuznetsova et al., 2020). In general, the image recognition process involves image acquisition, image preprocessing, feature extraction, and classifier design. As research progresses, intelligent learning and analysis methods have begun to be applied to pipeline image recognition. Technologies such as image processing and neural networks are employed to automatically extract features related to pipeline blockages, deformations, etc., which are then fed into a classifier for training, enabling the automatic identification of pipeline images. For example, Lang and others proposed a method based on multi-level feature fusion and multi-scale GhostNet. By employing the Adaptive Spatial Feature Fusion method to integrate various features and utilizing the Multi-Level Feature Fusion Multi-Scale GhostNet method, the accuracy of pipeline corrosion defect recognition in Magnetic Flux Leakage images is improved (Lang and Han, 2022). Zhang and others, by combining computer vision technology with traditional image processing techniques, have developed a wall-climbing robot with weld seam tracking functionality. Utilizing algorithms for weld seam recognition and centerline extraction, this robot can perform rapid non-destructive testing of the surface weld seams inside pressure pipelines (Zhang et al., 2023). Suyama and others propose a non-destructive testing method supporting radiographic images, aimed at detecting weld joints in petroleum pipelines. The proposed method extracts pixel windows from the pipeline area in the radiographic images and applies a deep neural network model to identify windows corresponding to weld joints (Suyama et al., 2019). Xu and others propose a deep learning object detection framework based on YOLOv5 and CNN models. This framework initially employs YOLOv5 for the classification of targets in Magnetic Flux Leakage (MFL) images of pipelines. Subsequently, based on the classification results, features containing defects are input into a CNN-based regression model, enabling the simultaneous identification of targets in MFL pseudo-color images and the depth of metal loss (Xu and Liu et al., 2023). Despite the numerous studies and analyses conducted on various types of pipeline images, the proposed algorithms are limited to specific image categories due to significant differences among different types of pipeline images. Issues such as low database generality and poor model transferability exist. Additionally, there is relatively limited research on the recognition and classification of subsurface pipe images in saline-alkali land. Training a network from scratch requires a large dataset, and the training process is challenging. On the other hand, although existing methods for pipeline image classification have achieved certain results in identifying various types of pipeline issues, they generally lack a mechanism for fine-grained assessment of the severity of pipeline problems. This undoubtedly restricts the practical applicability and effectiveness of these methods. Therefore, how to overcome the difficulty of network training and develop new methods capable of fine-grained assessment of the severity of pipeline issues remains a crucial research challenge we are currently facing.

Addressing the aforementioned issues, this paper investigates and proposes a hierarchical classification method for subsurface pipe images in saline-alkali land based on ResNet18 transfer learning. By introducing transfer learning strategies (Ding et al., 2018), the complexity of network training has been significantly reduced, leading to an enhanced performance of the model in recognizing features of subsurface pipe images. Additionally, this paper employs a hierarchical classification approach for a more refined categorization of subsurface pipe images. Specifically, this classification method allows for a more accurate and detailed assessment of the severity of subsurface pipe issues based on the extent of soil and salt crystal accumulation. This approach not only enhances our understanding of subsurface pipe issues but also provides crucial technical support and reference for subsequent subsurface pipe management and maintenance.

2. Materials and methods

2.1 Data acquisition and processing

2.1.1 Data acquisition

The subsurface pipe image dataset in this paper comprises three categories of images: normal pipe images, sediment accumulation images, and salt crystal accumulation images. Normal pipe images were collected under the condition of ensuring no blockage or damage in the drainage pipes, showing no anomalies in the internal space of the pipes. Due to the presence of numerous hydrophobic holes on saline-alkali land drainage pipes, fine sand and soil may inevitably enter the drainage pipes under the action of water flow. Additionally, as water flows through saline-alkali land, it absorbs a large amount of salt from the soil. After settling in the pipeline for a period, this can lead to the precipitation of salt crystals. Sediment and salt crystals adhere to the inner walls of the pipes, potentially causing blockages. Images of these locations where sediment accumulates and salt crystals precipitate were captured using specialized equipment, resulting in sediment accumulation images and salt crystal accumulation images. After image collection, the images of sediment and salt crystal accumulation were classified into three severity levels, as shown in Figure 1. This more detailed level of classification assists in a more accurate assessment of the severity of pipeline issues, enabling the implementation of more effective measures for governance and maintenance. It enhances the precision and efficiency of problem resolution.

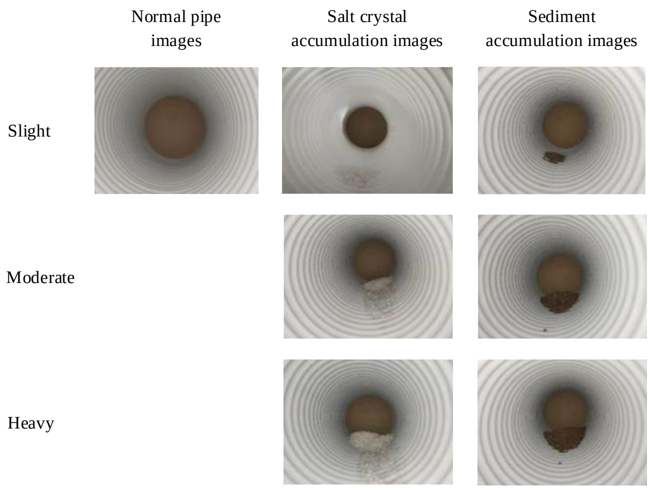

Fig. 1. Typical examples of the subsurface pipe image dataset.

2.1.2 Data enhancement

Subsurface pipes in saline-alkali land are typically located underground, and the internal environment is complex and variable. Collecting images of various subsurface pipe issues involves significant economic costs. Therefore, the sample size of the subsurface pipe image dataset is relatively small, making it challenging to meet the requirements of the network model. Additionally, as the image capture devices periodically take pictures and most areas of subsurface pipes in saline-alkali land do not have accumulation issues, the number of normal pipe images far exceeds that of other types, resulting in an imbalance in the dataset. In addressing the aforementioned issues, this study employed a data augmentation strategy to enhance the robustness of the model by expanding the sample size, aiming to achieve a more superior generalization effect.

The dataset was augmented using techniques such as width offset, height offset, horizontal and vertical flipping, cropping, and scaling. The augmented dataset comprises a total of 4711 images. The augmentation not only increases the diversity of the dataset but also contributes to enhancing the model's robustness, suppressing reliance on irrelevant features, and achieving better generalization. The augmented subsurface pipe image data was randomly selected in a 7:3 ratio for training and testing purposes. Specifically, the training set consists of 3298 images, and the testing set consists of 1413 images. The classification and quantity of the training and testing sets are detailed in Table 1. normal pipe images, sediment accumulation images, and salt crystal accumulation images

Tab. 1. The augmented dataset of dark tube images after data augmentation.

	Severity level	Image count	Training set count	Testing set count
Normal pipe images		736	515	221
Sediment accumulation images	Slight	628	440	188
	Moderate	652	456	196
	Heavy	663	464	199
Salt crystal accumulation images	Slight	700	490	210
	Moderate	688	482	206
	Heavy	644	451	193

2.2 Model architecture

2.2.1 ResNet18 network

ResNet18 is a deep convolutional neural network (Topaloglu et al., 2023; Chen et al., 2022), and its efficiency stems from the design of its residual block structure. From Figure 2, it can be seen that the block introduces skip connections, allowing the network to more easily learn residuals. In a flat network, information can only be transmitted through layers, whereas in a residual network, skip connections enable information to pass directly between different layers, effectively addressing issues such as gradient vanishing and exploding. Each block consists of a series of convolutional layers, which perform operations such as convolution, batch normalization, and activation functions (such as ReLU) on the input data to capture more advanced feature representations.

The ResNet network adds the input and output vectors of a block using a residual connection, and activates them using the ReLU function to obtain the feature value output of that block (Zhu et al., 2020; Ren and Mosavat et al., 2021). The calculation of this feature value output is given by Equation (1). This design ensures that as the network deepens, it does not introduce additional parameters or computational complexity.

$$y = F\left(x, \{W_i\}\right) + W_s x \tag{1}$$

where x and y represent the input and output vectors of a block in the ResNet network, respectively; $F(x, \{W_i\})$ represents a fully connected network, i.e., the residual mapping that the block aims to fit; W_s represents the linear mapping when matching the dimensions of the input and output vectors of that block.

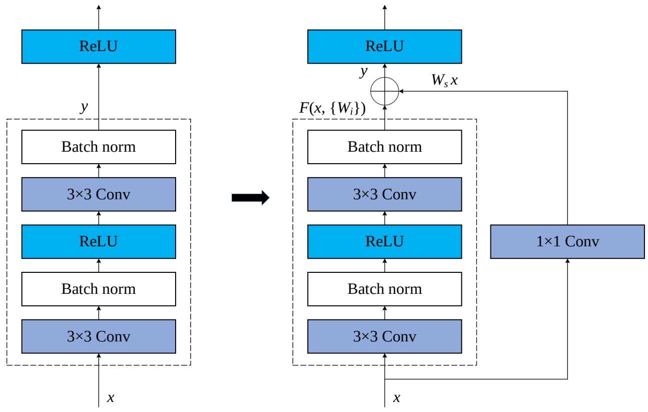

Fig. 2. Comparison between planar networks and residual networks.

2.2.1 Transfer learning

Deep Convolutional Neural Networks (DCNNs) typically require large annotated image datasets to reach the upper limit of classification accuracy. However, acquiring and annotating subsurface pipe image datasets for saline-alkali land is time-consuming and labor-intensive. In such cases, transfer learning can be employed using pre-trained classical DCNN models. Transfer learning, as an optimization technique, allows the beneficial information, such as the learned model structure and parameter weights of a convolutional neural network in one task, to be transferred to the pipeline detection task (Minoofam et al., 2021). This significantly accelerates the model construction process, reduces the complexity of network training, and effectively addresses the challenges arising from limited internal image data within the pipeline. This not only effectively utilizes the learning outcomes from the previous task during model transfer but also provides an efficient approach to handle relatively small-scale internal pipeline image data.

Figure 3 depicts the overall process of transfer learning on the subsurface pipe images. Before applying the pre-trained deep learning model to the subsurface pipe image dataset, modifications to the network architecture are necessary to adapt to the specific features of this dataset. After adjusting the network architecture, the obtained deep learning model is trained to optimize its performance on the subsurface pipe image task. The model training process is illustrated by equations (2) and (3):

$$T_S \leftarrow f(w_S, b_S) D_S \tag{2}$$

$$T_T \leftarrow f(w_S, b_S) D_T \tag{3}$$

where T_S is the source domain task, T_T is the target domain task, $f(w_S,$

b_S) represents the knowledge acquired by the network model on the source domain dataset, D_S is the source domain sample, and D_T is the target domain sample.

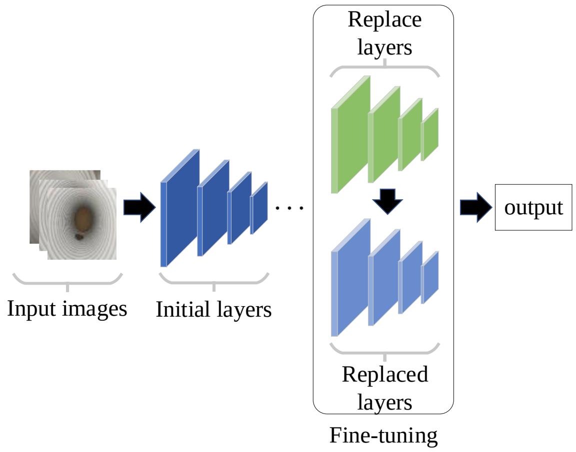

Fig. 3. Deep learning network transfer learning flowchart.

During the training process, the model parameters are optimized using gradient descent to enhance its generalization ability on the target task. Gradient descent method generally updates parameters along the opposite direction of the gradient to fine tune the network model and reduce the loss function. Gradient descent and the loss function are represented as Equation (4) and Equation (5), respectively:

$$w_{t+1} = w_t - l \times \frac{m_t}{1-\beta_1 t} / \sqrt{\frac{v_t}{1-\beta_2 t}} \tag{4}$$

$$H(y^-, y) = -\sum y^- \times \log(y) \tag{5}$$

where w_t represents the parameters at time t, m_t is the first-order moment, v_t is the second-order moment, β_1 and β_2 are the optimizer's parameters, y^- is the actual label of the sample, y is the model's predicted probability distribution, and H represents the cross-entropy loss. The cross-entropy loss penalizes the model for incorrect predictions of the true class by comparing the model's output with the ground truth.

2.2.3 Hierarchical classification method for subsurface pipes image based on ResNet18 transfer learning

This paper proposes a hierarchical classification method for subsurface pipe image based on ResNet18 transfer learning, aiming to enhance the accuracy and generalization capability of image classification. The introduction of transfer learning strategies significantly streamlines the network training process and enhances the model's ability to recognize features in subsurface pipe images. Simultaneously, employing a hierarchical classification approach for subsurface pipe images allows for a more precise assessment of the severity of saline-alkali land subsurface pipe issues based on the degree of soil and salt crystal accumulation. The approach proposed in this paper is illustrated in Figure 4 and mainly consists of three parts: image preprocessing, modify network architecture, and training and testing the network.

1) Image preprocessing: In the image preprocessing stage, various image augmentation methods such as horizontal flipping, vertical flipping, random rotation, size adjustment, and random brightness are employed to increase the number of samples in the dataset. Subsequently, the dataset is divided into a training set and a test set, with 70% of the images from each category used for training the network and 30% for testing the network. Meanwhile, automatic image annotation is performed based on the naming of the folders containing the subsurface pipe images. Additionally, image sizes are adjusted to meet the input requirements of the neural network.

2) Modify network architecture: To adapt to the characteristics of the subsurface pipe image dataset in saline-alkali land, adjustments were made to the network architecture of the pre-trained ResNet18 model. The original structure of ResNet18 employs a Global Average Pooling Layer in the last layer, followed by a fully connected layer with 1000 nodes to accommodate the 1000 categories of the ImageNet dataset. In this approach, the existing structure replaces the fully connected layer connected to the Global Average Pooling Layer with a new fully connected layer. The new fully connected layer consists of 7 nodes, corresponding to the image categories in the subsurface pipe image dataset.

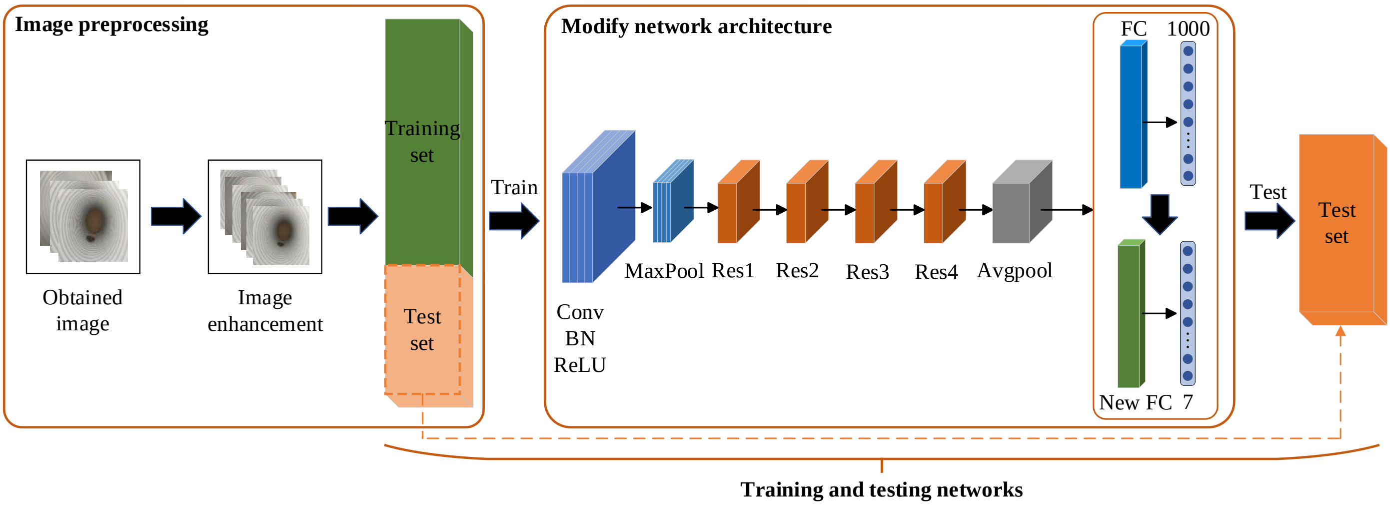

Fig. 4. Flowchart of the hierarchical classification method for subsurface pipe image based on ResNet18 transfer learning.

3) Training and testing the network: During the network training phase, we adjusted hyperparameters such as epochs, batch size, learning rate, optimizer, and loss function based on server performance and network structure. Through gradient descent operations, the network gradually optimized weights on the training set to adapt to the characteristics of subsurface pipe images in saline-alkali land. In the testing phase, we applied the trained model to the test dataset, evaluating the model's performance on the test set, including metrics such as loss function value and accuracy.

3. Experimental Results and Analysis

To validate the effectiveness of the hierarchical classification method for subsurface pipe image based on ResNet18 transfer learning, this section compares the method with transfer learning using pre-trained models of AlexNet (Zhang et al., 2023), MobileNet_V3 (Liu et al., 2023), and ShuffleNet_V2 (Chen et al., 2022). The dataset used in this study comprises 4711 subsurface pipe images, primarily consisting of three categories of images, all captured in JPG format. The experimental environment includes an Intel Core (TM) i5—11300H CPU with a maximum frequency of 3.10GHz, 16GB of RAM, Windows 11 operating system, and PyCharm as the development environment.

3.1 Evaluation metrics for the model

To assess the results of subsurface pipe image recognition, a reliability analysis was conducted on the transfer learning model for subsurface pipe images. Common metrics used in the field of machine learning, especially in statistical classification problems, were employed to evaluate the performance of the model. Four evaluation metrics, including accuracy (ACC), precision (P), recall (R), and F1 score, were selected to measure the overall accuracy of the model. The confusion matrix was used to reflect the accuracy of each subsurface pipe image classification.

The accuracy (ACC) provides an intuitive representation of the proportion of correctly classified results for subsurface pipe images in the overall test set by the classification model.

$$ACC = \frac{TP + TN}{TP + TN + FP + FN} \tag{6}$$

Precision (P) represents the weighted average of precision rates (Pi) for different types of subsurface pipe images, where Pi indicates the proportion of correctly predicted instances in a particular type of subsurface pipe image out of all instances predicted as that type. Precision measures the model's ability to distinguish negative samples, with higher precision indicating stronger discrimination ability against negative samples.

$$P_i = \frac{TP_i}{TP_i + FP_i} \tag{7}$$

$$P = \frac{\sum_{i=1}^{L} P_i \times w_i}{|L|} \tag{8}$$

Recall (R) represents the weighted average of recall rates (Ri) for different types of subsurface pipe images, where Ri indicates the proportion of correctly predicted instances in a particular type of subsurface pipe image out of the total instances of that type. Recall measures the model's ability to distinguish positive samples, with higher recall indicating stronger discrimination ability against positive samples.

$$R_i = \frac{TP_i}{TP_i + FN_i} \tag{9}$$

$$R = \frac{\sum_{i=1}^{L} R_i \times w_i}{|L|} \tag{10}$$

where i represents a specific type of subsurface pipe image, L indicates the total number of categories of subsurface pipe images, $i \in [1, L]$, w represents the weight of a specific type of subsurface pipe image in the overall dataset.

F1 is the weighted average of precision (P) and recall (R), considering both precision and recall. Its values range from 0 to 1, where 1 represents the best model output, and 0 represents the worst model output.

$$F_1 = \frac{2P \times R}{P + R} \tag{11}$$

After classifying subsurface pipe images, using a Confusion Matrix provides a clear and intuitive way to distinguish how the model predicts and classifies different types of subsurface pipe images. As shown in Table 2, each column of the confusion matrix represents instances in a predicted class, and each row represents instances in an actual class. The four fundamental indicators are TP (True Positive), FP (False Positive), FN (False Negative), and TN (True Negative). TP represents the number of instances of a specific type of subsurface pipe image that are correctly predicted, FP represents the number of instances of other types of subsurface pipe images predicted as a specific type, FN represents the number of instances of a specific type of subsurface pipe image incorrectly predicted as other types, and TN represents the number of instances of other types of subsurface pipe images predicted correctly as other types.

Tab. 2. Confusion matrix.

Confusion matrix		Predictive value	
		Positive	Negative
True value	True	TP	FN
	False	FP	TN

3.2 Comparison of model training results

In Figure 5, we present the accuracy performance of four different pre-trained models in the subsurface pipe image recognition task. The data in the graph indicates that the deep learning transfer model based on ResNet18 outperforms other models in terms of accuracy (ACC), achieving a classification accuracy of 90.52%. In comparison, the accuracy of other deep learning transfer models is below this level, with values of 88.39%, 88.8%, and 58.67%, respectively. These data suggest that the deep learning transfer model based on ResNet18 exhibits higher precision and reliability in classifying subsurface pipe images.

The accuracy curve and training loss curve of the deep learning transfer model based on ResNet18 on the training set are shown in Figure 6. From the graph, it can be observed that the model's accuracy and training loss converge rapidly. This is attributed to the fact that the deep learning transfer model based on ResNet18 is pretrained on the source domain, inheriting the parameters of the feature extraction part of ResNet18. As a result, it achieves high accuracy in a relatively small number of iterations and tends to stabilize.

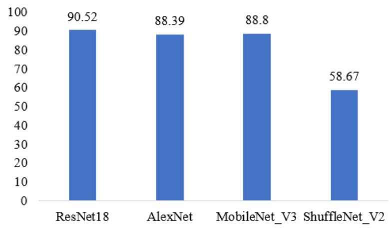

Fig. 5. Comparison of accuracy in classification and recognition of dark tube images.

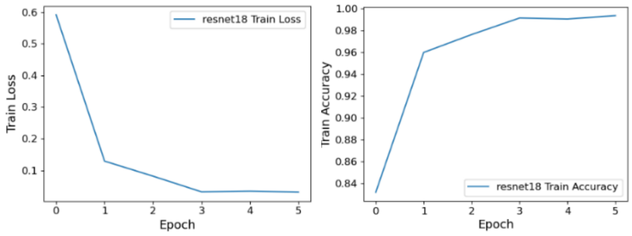

Fig. 6. Training process of deep learning transfer model based on ResNet18.

By employing precision (P), recall (R), and F1 score, we further compared the performance of the deep learning transfer model based on the ResNet18 network with other deep learning transfer models on the overall dataset. The deep learning transfer model based on ResNet18 network performs well in terms of accuracy, reaching 90.70%. In contrast, the precision of other deep learning transfer models was lower, ranging from a maximum of 90.42% to a minimum of 65.05%. This indicates that the deep learning transfer model based on the ResNet18 network can more accurately identify true positive samples when classifying subsurface pipe images.

In terms of recall, the deep learning transfer model based on the ResNet18 network also performed exceptionally well, reaching 90.69%. The recall of other deep learning transfer models was lower, ranging from a maximum of 90.41% to a minimum of 59.65%. This indicates that the deep learning transfer model based on the ResNet18 network can more comprehensively identify true positive samples.

Finally, a comprehensive evaluation of the classifier's performance was conducted using the F1 score, which is the harmonic mean of precision and recall. The deep learning transfer model based on the ResNet18 network achieved an F1 score of 90.69%. The F1 scores of other deep learning transfer models were lower, ranging from a maximum of 90.41% to a minimum of 55.19%. This indicates that the deep learning transfer model based on the ResNet18 network has overall better classification performance.

In summary, the deep learning transfer model based on the ResNet18 network outperforms other deep learning transfer models in terms of precision, recall, and F1 score. This indicates that the model has a higher true positive rate, a higher positive predictive value, and overall superior classification performance.

Tab. 3. Comparison of precision, recall, and F1 indicators.

Classification model	P/%	R/%	F1/%
ResNet18	90.70	90.69	90.69
AlexNet	88.47	88.42	88.43
MobileNet_V3	90.42	90.41	90.41
ShuffleNet_V2	65.05	59.65	55.19

In Figure 7(a), it can be observed that the deep learning transfer model based on ResNet18 correctly identifies 186 images in the classification of images with moderate salt crystal accumulation, 182 images in the classification of images with moderate sediment accumulation, and 190 images in the classification of images with severe sediment accumulation.

However, in Figures 7(b) and (c), when using the deep learning transfer models based on AlexNet and MobileNet_V3, the classification accuracy for images with moderate salt crystal accumulation, moderate sediment accumulation, and severe sediment accumulation is lower compared to the transfer model based on ResNet18. On the other hand, in Figure 7(d), the deep learning transfer model based on ShuffleNet_V2 exhibits significantly lower accuracy in the classification of subsurface pipe images, except for normal pipe images and images with severe salt crystal accumulation, when compared to the model based on ResNet18.

In summary, the deep learning transfer model based on ResNet18 demonstrates higher stability in classifying subsurface pipe images.

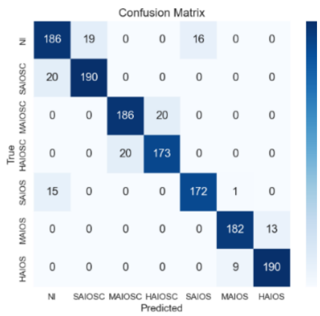

(a) Confusion Matrix Based on ResNet18

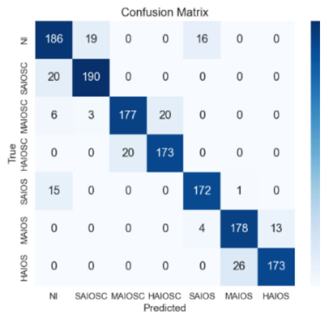

(b) Confusion Matrix Based on AlexNet

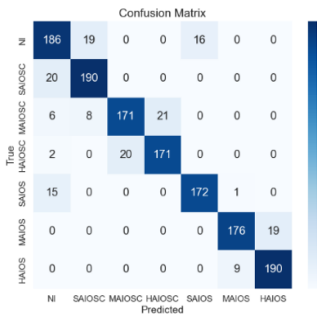

(c) Confusion Matrix Based on MobileNet_V3

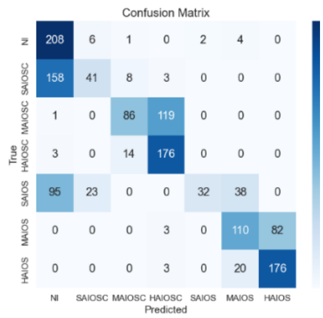

(d) Confusion Matrix Based on ShuffleNet_V2

Fig. 7. Comparison of confusion matrix images in deep learning transfer models for subsurface pipe images. NI(normal pipeline image), SAIOSC(slight accumulation image of salt crystals), MAIOSC(moderate accumulation image of salt crystals), HAIOSC(heavy accumulation image of salt crystals), SAIOS(slight accumulation image of sediment), MAIOS(moderate accumulation image of sediment), HAIOS(heavy accumulation image of sediment)

4. Summary

The hierarchical classification method for subsurface pipe image based on ResNet18 transfer learning, proposed in this paper, has achieved significant success in addressing challenges such as difficulties in collecting subsurface pipe images in saline-alkali land, limited sample size, and the lack of a fine evaluation mechanism. Through transfer learning, we successfully reduced the sample size requirement for network training and improved the model's performance in recognizing subsurface pipe image features. Additionally, the adoption of hierarchical classification allows for a more refined categorization of subsurface pipe images, effectively evaluating the degree of sediment and salt crystal accumulation. Compared to other models, this approach not only demonstrates superior recognition accuracy but also exhibits higher stability across various types of subsurface pipe images. This method provides an effective solution for the rapid and intelligent recognition of underground salt discharge pipe images. Future research directions may include further optimizing model performance and exploring its applicability in other geological environments.

Acknowledgements

The authors would like to acknowledge financial support provided by the National Natural Science Foundation of China (62001263), the Key research projects of Qingdao Science and Technology Plan (22-3-3-hygg-30-hy), and the Natural Science Foundation of Shandong Province (ZR2021MF024).

References

Zhang, P., Bing, X., Jiao, L., et al., 2022, Amelioration effects of coastal saline-alkali soil by ball-milled red phosphorus-loaded biochar. J. Chemical Engineering Journal. 431(1).

Cui, C., Shen, J., Zhu, Y., et al., 2023, Bioremediation of phenanthrene in saline-alkali soil by biochar-immobilized moderately halophilic bacteria combined with Suaeda salsa L. J. Science of The Total Environment. 880.

Chen, Q., Cao, X., Li, Y., et al., 2022, Functional carbon nanodots improve soil quality and tomato tolerance in saline-alkali soils. J. Science of The Total Environment. 830.

Liu, Y., Ao, C., Zeng, W., et al., 2021, Simulating water and salt transport in subsurface pipe drainage systems with HYDRUS-2D. J. Journal of Hydrology. 592.

Yang, Y., Zhu, Y., Wu, J., et al., 2022, Development and application of a new package for MODFLOW-LGR-MT3D for simulating regional groundwater and salt dynamics with subsurface drainage systems. J. Agricultural Water Management. 260.

Piciarelli, C., Avola, D., Pannone, D., et al., 2018, A vision-based system for internal pipeline inspection. J. IEEE Transactions on Industrial Informatics. 15(6), 3289-3299.

Xu, H., Yang, Y., Gao, B., et al., 2022, Multi-layer feature boosting framework for pipeline inspection using an intelligent pig system. J. IEEE Transactions on Industrial Informatics. 19(7), 8406-8417.

Huang, Y., Qin, G., Yang, M., 2023, A risk-based approach to inspection planning for pipelines considering the coupling effect of corrosion and dents. J. Process Safety and Environmental Protection. 180, 588-600.

Yang, L., Wang, Z., Gao, S., et al., 2019, Magnetic flux leakage image classification method for pipeline weld based on optimized convolution kernel. J. Neurocomputing. 365, 229-238.

Liu, X., Jiao, L., Li, L., et al., 2020, Deep multiview union learning network for multisource image classification. J. IEEE Transactions on Cybernetics. 52(6), 4534-4546.

Kuznetsova, A., Rom, H., Alldrin, N., et al., 2020, The open images dataset v4: Unified image classification, object detection, and visual relationship detection at scale. J. International Journal of Computer Vision. 128(7), 1956-1981.

Lang, X., Han, F., 2022, MFL image recognition method of pipeline corrosion defects based on multilayer feature fusion multiscale ghostnet. J. IEEE Transactions on Instrumentation and Measurement. 71.

Zhang, Y., Guan, E., Li, P., et al., 2023, An automated nondestructive testing system for the surface of pressure pipeline welds. J. Journal of Field Robotics. 40(8), 1927-1944.

Suyama, F.M., Delgado, M.R., Silva, R.D., et al., 2019, Deep neural networks based approach for welded joint detection of oil pipelines in radiographic images with Double Wall Double Image exposure. J. Ndt & E International. 105, 46-55.

Xu, Z., Liu, K., Gu, B., et al., 2023, Image recognition model of pipeline magnetic flux leakage detection based on deep learning. J. Corrosion Reviews. 41, 689-701.

Ding, Z., Shao, M., Fu, Y., 2018 Incomplete multisource transfer learning. J. IEEE transactions on neural networks and learning systems. 29(2), 310-323.

Topaloglu, I., Barua, P.D., Yildiz, A.M., et al., 2023. Explainable attention ResNet18-based model for asthma detection using stethoscope lung sounds. J. Engineering Applications of Artificial Intelligence. 126.

Chen, Z., Jiang, Y., Zhang, X., et al., 2022. ResNet18DNN: prediction approach of drug-induced liver injury by deep neural network with ResNet18. J. Briefings in Bioinformatics. 23(1).

Zhu, H., Sun, M., Fu, H., et al., 2020. Training a seismogram discriminator based on ResNet. J. IEEE Transactions on Geoscience and Remote Sensing. 59(8), 7076-7085.

Ren, X., Mosavat-Jahromi, H., Cai, L., et al., 2021. Spatio-temporal spectrum load prediction using convolutional neural network and ResNet. J. IEEE Transactions on Cognitive Communications and Networking. 8(2), 502-513.

Minoofam, S.A.H., Bastanfard, A., Keyvanpour, M.R., 2021, TRCLA: a transfer learning approach to reduce negative transfer for cellular learning automata. J. IEEE transactions on neural networks and learning systems. 34(5), 2480-2489.

Zhang, C., Zhang, H., Tian, F., et al., 2023. Research on sheep face recognition algorithm based on improved AlexNet model. J. Neural Computing and Applications.

Liu, Y., Wang, Z., Wang, R., et al., 2023. Flooding-based MobileNet to identify cucumber diseases from leaf images in natural scenes. J. Computers and Electronics in Agriculture. 213.

Chen, Z., Yang, J., Chen, L., et al., 2022 Garbage classification system based on improved ShuffleNet v2. J. Resources, Conservation and Recycling. 178.

Zhaopeng Deng received his Ph.D from Shandong University of Science and Technology, China in 2019. His major research interests include image processing and machine vision. Currently he is a teacher in Qingdao University of Technology. His major research interests include intelligent control, image processing, machine vision and pattern recognition. He has published over 6 research papers in international journals, and conferences.

Shuangyang Han is currently pursuing a master's degree in Information and Control Engineering at Qingdao University of Technology. He obtained a bachelor's degree from Tianjin Sino German University of Applied Technology in 2020. His main research areas are computer vision, image processing, image recognition, image classification, and deep learning.

Wen Hao is currently pursuing his MEng study at the Institute of Information Control and Engineering, Qingdao University of Technology, Qingdao, China. He obtained his BS degree from Tongda College, Nanjing University of Posts and Telecommunications, China in 2023. His main research direction is saline alkali underground pipe robots

Guangfen Zhang received her Master's degree in 2014 from Tianjin University of Finance and Economics. Currently, she is an associate professor in Qingdao Huanghai University. Her research interests include big data analysis and artificial intelligence.